

# UC San Diego

## UC San Diego Electronic Theses and Dissertations

### Title

Genetic modification and mutant construction for proteins involved in the CO2 signaling pathway of Arabidopsis thaliana

### Permalink

<https://escholarship.org/uc/item/4pp2f9p0>

### Author

Bosmans, Krystal Carson

### Publication Date

2022

Peer reviewed|Thesis/dissertation

UNIVERSITY OF CALIFORNIA SAN DIEGO

Genetic modification and mutant construction for proteins involved in the CO<sub>2</sub> signaling pathway of *Arabidopsis thaliana*

A thesis submitted in partial satisfaction of requirements  
for the degree of Master of Science

in

Biology

by

Krystal Bosmans

Committee in charge:

Professor Julian I Schroeder, Chair  
Professor Mark Estelle  
Professor Alisa Huffaker

2022

Copyright  
Krystal Bosmans, 2022  
All rights reserved

The Master's Thesis of Krystal Bosmans is approved, and it is acceptable in quality and form for publication on microfilm and electronically.

University of California San Diego

2022

## TABLE OF CONTENTS

<b>THESIS APPROVAL PAGE</b> .....	iii
<b>TABLE OF CONTENTS</b> .....	iv
<b>LIST OF FIGURES</b> .....	vi
<b>LIST OF TABLES</b> .....	vii
<b>ACKNOWLEDGMENTS</b> .....	viii
<b>ABSTRACT OF THE THESIS</b> .....	ix
<b>INTRODUCTION</b> .....	1
<b>RESULTS</b> .....	9
<i>1.1 Genotyping and isolation of the cbc1/cbc2/ht1(A109V) triple mutant</i> .....	9
<i>1.2 Whole leaf gas exchange experiments of the cbc1/cbc2/ht1(A109V) triple mutant</i> .....	13
<i>1.3 Construction of MPK12 and CBC1 GFP vectors</i> .....	16
<i>1.4 Whole leaf gas exchange experiments of pGC1:CBC1(T256A/S280A)-GFP/cbc1cbc2 and pGC1:CBC1-GFP/cbc1cbc2 mutant lines</i> .....	23
<i>1.5 Whole leaf gas exchange experiments of pGC1:MPK12-GFP/mpk12 and pGC1:MPK12(K70R)-GFP/mpk12 mutant lines</i> .....	25
<b>DISCUSSION</b> .....	28
<b>MATERIALS AND METHODS</b> .....	39
<i>1.1 Plant growth conditions</i> .....	39
<i>1.2 Hygromycin selection assays</i> .....	40
<i>1.3 Genome extraction from plants</i> .....	41
<i>1.4 Crossing Arabidopsis thaliana samples</i> .....	42
<i>1.5 E. coli transformation</i> .....	43

<i>1.6 Cloning of MPK12 and CBC1 vectors</i> .....	44
<i>1.7 Agrobacterium tumefaciens transformation</i> .....	46
<i>1.8 Arabidopsis thaliana transformation with A. tumefaciens vectors via floral dipping</i> .....	47
<i>1.9 Confocal microscopy imaging</i> .....	48
<i>1.10 Li-COR gas exchange experiments</i> .....	49
<b>WORKS CITED</b> .....	50

## LIST OF FIGURES

Figure 1. Polymerase chain reaction and HT1 genetic sequencing used to identify <i>cbc1/cbc2/ht1(A109V)</i> triple mutant samples.....	10
Figure 2. Stomatal conductance comparisons of Col-0, <i>cbc1/cbc2</i> , <i>ht1(A109V)</i> , and <i>cbc1/cbc2/ht1(A109V)</i> .....	15
Figure 3. Construction plan for MPK12 and CBC1 GFP vectors.....	18
Figure 4. Confocal results of guard cell GFP fluorescence in a <i>pGCI:CBC1(T256A/S280A)-GFP/cbc1cbc2</i> candidate.....	19
Figure 5. Stomatal conductance comparisons of WT, <i>cbc1/cbc2</i> , <i>pGCI:CBC1(T256A/S280A)-GFP/cbc1cbc2</i> and <i>pGCI:CBC1-GFP/cbc1cbc2</i> .....	24
Figure 6. Stomatal conductance comparisons of WT, <i>mpk12</i> , <i>pGCI:MPK12-GFP/mpk12</i> and <i>pGCI:MPK12(K70R)-GFP/mpk12</i> .....	27

## LIST OF TABLES

Table 1. PCR primers used for construction of <i>cbc1/cbc2/ht1(A109V)</i> .....	11
Table 2. Length of expected DNA fragment using primers from Table 1.....	12
Table 3. Primers used for cloning of GFP vectors using USER and SLiCE cloning systems .....	20
Table 4. Length of expected DNA fragment using primers from Table 3.....	21
Table 5. Clones, plasmids, and vectors used from or added to the Julian Schroeder's lab stocks.....	22



## ACKNOWLEDGMENTS

I would like to thank Dr. Julian Schroeder for providing me the opportunity to be able to work in his lab for the last three and a half years and for serving as the chair of my committee. I joined the lab in my third year of undergrad and have had the best time serving with all of my peers who are all pursuing their own unique projects within the lab. I thank Dr. Schroeder for all of his support and advice given during my time, especially in the last year. Your feedback as I wrote my thesis was critical for its development. Thank you to the other members of my committee Dr. Alisa Huffaker and Dr. Mark Estelle for taking the time out of your busy schedules to serve on my master's committee.

I would also like to thank my immediate mentor Dr. Yohei Takahashi. I will always be grateful for how patient you were when I was still learning the ropes, how you were always willing to answer any questions I had, and how you provided as much guidance as you could even after you traveled back to Japan. Your mentorship was fundamental in my experience at the lab and I will always be thankful for all of your help, encouragement, passion, and guidance.

Finally, to my parents Tom and Renee, my partner Jordan, my lab bestie Bryn, and my friends Kara, Kelsey, Kat, Kayla, Sarah, Luna, and Andrea, thank you for being there for me throughout this whole journey and reminding me that I was capable and never letting me give up. This is for you all, I hope that I made you guys proud.

Material in this thesis has been submitted for publication of the material as it may appear in Science Advances, 2022, Bosmans, Krystal; Yohei Takahashi., Po-Kai Hsu, Karnelia Paul, Chung-Yueh Yeh, Yuh-Shuh Wang, Dmitry Yarmolinsky, Maija Sierla, Triin Vahisalu, Jaakko Kangasjarvi, Hannes Kollist, Li Zhang, Thien Trac, and Julian I. Schroeder. The thesis author was the primary investigator and author of this paper.

## ABSTRACT OF THE THESIS

Genetic modification and mutant construction for proteins involved in the CO<sub>2</sub> signaling pathway of *Arabidopsis thaliana*

by

Krystal Bosmans

Master of Science in Biology

University of California San Diego, 2022

Professor Julian Schroeder, Chair

As atmospheric carbon dioxide levels continue to rise, agricultural yields will be impacted worldwide. Our laboratory obtained evidence that specific MAPKs inhibit the activity of HT1, a negative regulator of CO<sub>2</sub>-induced stomatal closure. The findings showed that HT1 can phosphorylate CBC1/2 but not whether HT1 regulates CBC1/CBC2's activity. This study

analyzed stomatal conductance responses to changing CO<sub>2</sub> levels with a *cbc1/cbc2* double knockout line, a dominant *ht1(A109V)* line with a permanently active HT1 protein, and a *cbc1/cbc2/ht1(A109V)* triple mutant line with knocked out CBC1 and CBC2 genes and a constantly active HT1 protein. The *cbc1/cbc2/ht1(A109V)* mutant showed stomatal conductance values similar to *cbc1/cbc2* samples, not *ht1(A109V)*. The results suggest that the CBC1/CBC2 are epistatic to and function downstream of HT1 in the signaling pathway. Next, mutant lines of *pGCI:MPK12(K70R)-GFP/mpk12*, with a K70R mutation in MPK12, and *pGCI:MPK12-GFP/mpk12*, a rescue line, both showed stomatal conductance responses similar to Col-0. Meanwhile, *mpk12* samples showed responses to changes in CO<sub>2</sub> but higher stomatal conductance levels compared to Col-0. The data suggests that the kinase activity of MPK12 is not required to inhibit HT1. The final experiments used a line with two mutations in mapped HT1-mediated CBC1 phosphorylation sites, *pGCI:CBC1(T256A/S280A)-GFP/cbc1cbc2*, showed stomatal conductance similar to the *cbc1/cbc2* samples while the rescue line *pGCI:CBC1-GFP/cbc1cbc2* with a wildtype CBC1 gene, showed stomatal responses similar to Col-0. This suggests that the two mutated sites could be important for HT1 phosphorylation. The information gathered here can contribute to developing agricultural lines that can withstand rising levels of CO<sub>2</sub>.

## INTRODUCTION

Plants have been a crucial organism that impacts the living world in multiple ways such as supplying the atmosphere with oxygen through photosynthesis and acting as a food source for human and domestic animal consumption. As primary producers, it is important that plants are not exposed to stressful environmental conditions so that their growth is not negatively affected. Plants can experience stress on a daily basis from a number of abiotic sources including temperature, salinity, drought, and toxic metals in addition to biotic stresses like predation from herbivores (Gull et al., 2019). The human population has been increasing at a rapid rate since the Industrial Revolution, when the global birth rate became significantly larger. Furthermore, the global death rate declined as a result of improved technology that lead to lower mortality rates and longer life expectancy (Bongaarts, 2009). With a continuously growing population, it is important that the world can maintain a level of primary produce production that supports the global population.

Also increasing globally is the concentration of carbon dioxide (CO<sub>2</sub>) within the atmosphere which recently has been recorded to be ~416 ppm (<https://keelingcurve.ucsd.edu>). Over the past 1 million years and before the industrial revolution, the atmospheric CO<sub>2</sub> concentration would fluctuate between 150-280 ppm but it had not surpassed 300 ppm until the Industrial Revolution. This is critical because carbon dioxide can absorb the infrared radiation (heat) of sunlight and trap it within Earth's atmosphere, this results in an overall increase in temperature (Callendar, 1938). Callendar's study also noted that there would be more concentrated radiation absorption in the lower layers of the atmosphere following an increase in atmospheric carbon dioxide. Recently, the Intergovernmental Panel on Climate Change (IPCC) stated that since the middle of the 20<sup>th</sup> century, human activities were likely responsible for the

observed increase in global temperatures (IPPC, 2014). Rising levels of carbon dioxide and increasing temperatures are just two products of climate change that are affecting our biosphere, in addition to more frequent extreme weather patterns, ocean acidification, and rising sea levels (USGCRP, 2017).

Plants are sessile organisms, meaning that they cannot move freely when their environment no longer suits them, they must either adapt to the abiotic and biotic challenges they are presented with or cease to survive (Gull et al., 2019). Water use and gas exchange are two plant activities that are crucial for survival and can be affected by changes in the environment. Plants have a cellular complex known as a stomate that resembles a pore on their leaves that responds to such changes, so they can continue to survive (Zhang et al., 2018). It is the function of stomata to maintain a level of gas exchange that is optimal for the needs of photosynthesis by keeping the aperture of the stomatal pore at an appropriate width so there is balance between water loss from transpiration and exchange of carbon dioxide and oxygen (Darwin, 1898). Each stomatal pore is surrounded by a pair of guard cells that regulate the size of the stomatal aperture to allow optimal amounts of carbon dioxide to enter the intracellular space of leaves from the atmosphere (Zhang et al., 2018). The pressure exerted on the cell wall of guard cells by the intercellular fluid is affected by changes in ion and solute osmolarity and as a result influences stomatal aperture size (Ainsworth and Rogers, 2007). Because changes in carbon dioxide concentration influence the width of stomatal apertures, it is an important subject in relation to the agriculture industry. Elevated carbon dioxide levels could lead to an increase in plant biomass depending on the conditions. An increase in plant production may positively affect crop yields because plants would have access to more carbon dioxide for use in sugar production. However, a previous study using soybeans found that high amounts of atmospheric carbon

dioxide could not counteract the negative effects that the plants experienced when they were exposed to high temperatures and drought-like conditions (Gray et al., 2016). This study also concluded that due to abiotic factors such as changes in water availability and temperature associated with climate change, it is difficult to determine overall specifically how crop yields will be affected.

In environments with low concentrations of carbon dioxide, the stomatal aperture widens to allow more carbon dioxide enter while in environments with high concentrations of carbon dioxide, the stomatal aperture narrows and allows less carbon dioxide to enter even if the light conditions are optimal for photosynthesis (Zhang et al., 2018). As a result of long-term exposure to higher than ambient atmospheric carbon dioxide levels, plant stomata become narrower, the overall stomatal density on leaves is reduced, the intracellular temperatures of leaves increase, and water-use efficiency is affected (Hetherington and Woodward, 2003). If stomata remain closed it is possible that the plant could die from overheating or from lack of access to the carbon dioxide needed to build sugars for growth and development. Multiple studies have predicted or observed a decrease in the crop yield of grains when they are exposed to higher temperatures or drought, an increasingly common occurrence as atmospheric carbon dioxide levels continue to rise (Parry, 2007; Hatfield, 2016; Shim et al., 2017).

With the looming threat of climate change, specifically rising carbon dioxide levels in our generation, there is a lot interest in understanding the signaling pathways that induce stomatal closure. The two main pathways being studied include one triggered by carbon dioxide levels and another triggered by production of the plant stress hormone abscisic acid (ABA) in response to drought conditions. This work described herein will be focusing on the signaling pathway that is induced by changes in carbon dioxide levels. This pathway starts with the entry of CO<sub>2</sub> into the

intracellular space of the leaf through the opening of the stomatal pore (Zhang et al., 2018). The  $\text{CO}_2$  is then reversibly converted into bicarbonate ( $\text{HCO}_3^-$ ) by multiple beta-carbonic anhydrases ( $\beta$ -CA) (Hu et al., 2010). There are three major known gene families of carbonic anhydrases, alpha, beta, and gamma, all of which have homologs in our plant model system, *Arabidopsis thaliana* (Hewett-Emmett and Tashian, 1996). Specifically, the  $\beta\text{CA1}$  and  $\beta\text{CA4}$  carbonic anhydrases expressed in guard cells convert the entering carbon dioxide into protons and bicarbonate, the latter of which stimulates the downstream signaling cascade that results in changes to the width of stomatal apertures (Hu et al., 2010, Xue et al., 2011).

The next protein involved in the carbon dioxide signaling pathway is a type of mitogen-activated protein kinase (MAPK) and in *A. thaliana*, the MPK12 and MPK4 genes/proteins mediate the stomatal  $\text{CO}_2$  response (Jakobson et al., 2016, Töldsepp et al., 2018). Previous studies with *MPK4-silenced Nicotiana tabacum* have shown stomata to have regular movements when exposed to ABA treatments but lacked stomatal closing in environments with high  $\text{CO}_2$  levels (Gomi et al., 2005, Hettenhausen et al., 2012, Marten et al., 2008). These observations lead to an interest to investigate whether the MPK4 protein had a similar role in *A. thaliana*. A double mutant where MPK4 was suppressed in guard cells while MPK12 was disrupted via a T-DNA insertion showed similar results, where ABA-induced stomatal closure was functioning, while stomatal responses to elevated carbon dioxide were impaired (Töldsepp et al., 2018). Additionally, *in vitro* experiments from this same study concluded that kinase activity from MPK4/MPK12 was not directly activated by bicarbonate levels suggesting that there is another component of the signaling pathway upstream of the MAP kinases (Töldsepp et al., 2018). MPK12 then goes on to inhibit the protein kinase high leaf temperature1 (HT1) by unknown

mechanisms which may then affect directly or indirectly two convergence of blue light and CO<sub>2</sub> (CBC1/2) kinases (Hörak et al., 2016; Hiyama et al., 2017).

MPK12 has previously been shown to interact with HT1 by inhibiting its activity (Jakobson et al., 2016). Jakobsen also found that HT1 has the ability to activate itself via autophosphorylation but is inhibited by active MPK12 *in vitro*. These observations were further confirmed in SDS page gel experiments that included wildtype HT1, kinase dead HT1, and multiple MPK12 proteins with varying levels of activity (Jakobson et al., 2016).

Experiments using mutant *A. thaliana* lines in two of seven known HT1 alleles (*ht1-2* and *ht1-3*) showed genetically dominant disruption of stomatal signaling induced by elevated CO<sub>2</sub> levels but similar stomatal aperture widths compared to wildtype following treatment with ABA indicating that it was only carbon dioxide-induced stomatal signaling that was impacted (Hashimoto-Sugimoto et al., 2016). An A109V mutation in HT1 resulted *in vitro* in a reduced ability of MPK12 to inhibit the autophosphorylation activity of HT1 so that it remains active, although there have not yet been any *in vivo* studies (Hörak et al., 2016). HT1 was shown *in vitro* to phosphorylate both wildtype CBC1/CBC2 and kinase dead CBC1/CBC2 proteins that lost their ability to autophosphorylate themselves or phosphorylate other proteins (Hiyama et al., 2017). However, the effect of this *in vitro* phosphorylation remains unknown. This same study also observed that CBC1/CBC2 did not phosphorylate HT1 despite the protein kinase activity of CBC1 and CBC2. The fact that HT1 can activate CBC1/CBC2 has led to hypotheses that CBC1/CBC2 could function in the same signaling pathway as HT1 and CBC1/CBC2 impact stomatal closure.

Downstream in the signaling pathway of CBC1/CBC2 is the S-type anion channel-associated 1 (SLAC1) protein that controls the efflux of ions that leave the guard cells, thereby



reducing the turgor pressure leading to a reduction in the stomatal aperture size. Some ions that have been suggested to be responsible for these fluctuations in the carbon dioxide signaling pathway include calcium ( $\text{Ca}^{2+}$ ) and potassium ( $\text{K}^+$ ) (Webb et al., 1996, Schroeder et al., 1984).

In guard cells, an influx of  $\text{K}^+$  via inward  $\text{K}^+$  channels is coupled with  $\text{H}^+$  extrusion that creates a current that contributes to the opening of stomata (Schroeder et al., 1984, Assmann et al., 1985, Schroeder et al., 1987). Changes in ion concentrations like these result in an osmotic influx of water into the guard cells that facilitates the opening of stomata via the resulting turgor pressure increase. A previous study found that in mutant *SLAC1* guard cells, the rate of stomatal opening was greatly reduced but not completely disrupted (Laanemets et al., 2013). CBC1/CBC2 are hypothesized to inhibit SLAC1 ion channels directly or indirectly by unknown mechanisms (Hiyama et al., 2017). SLAC1 influences changes in stomatal aperture but because there are so many signaling pathways that converge on SLAC1 it is unknown whether or how the two components interact (Hiyama et al., 2017).

There has been much research done on carbon dioxide-induced stomatal closure that is supported by genetic evidence, but the knowledge of what specific proteins interact and regulate targets in the signal transduction pathway is far from complete. While previous studies have shown that HT1 and CBC1/CBC2 interact *in vitro*, it is currently unknown if they indeed are in the same pathway and if CBC1/CBC2 functions downstream of HT1. One goal of this study was to determine through *in vivo* experiments whether the CBC1/CBC2 proteins act downstream of HT1 in the carbon dioxide-induced signal transduction pathway. Therefore, a *cbc1/cbc2/ht1(A109V)* triple mutant transgenic *A. thaliana* line was developed for use in stomatal conductance experiments to determine if CBC1/CBC2 are epistatic to HT1, which can be interpreted as CBC1 and CBC2 most likely acting downstream of HT1 in the carbon dioxide

signaling transduction pathway. Our hypothesis is that the mutated *ht1(A109V)* protein keeps stomata open through activation of CBC1/CBC2 and that its phenotype will be dependent on the existence of CBC1/CBC2 in the pathway. If the triple mutant exhibits a phenotype similar to the *cbc1/cbc2* double mutant instead of the *ht1(A109V)* phenotype, it would suggest that CBC1/CBC2 do function downstream of HT1.

Another goal of this study was to explore the importance of kinase activity in MPK12 and possible HT1 phosphorylation sites on CBC1. There have been preliminary experiments *in vitro* that suggest that the kinase activity of MPK12 might not be not required for its ability to mediate CO<sub>2</sub> signal transduction, but there have been no experiments that explore whether this is consistent *in vivo*. There has also been unpublished new research from our laboratory exploring possible phosphorylation sites for HT1 on the CBC1 protein. Mass spectrometry experiments were performed following *in vitro* phosphorylation assays that focused on CBC1 with and without the presence of bicarbonate. Comparing the two data sets, eight potential phosphorylation sites were identified as possible mutation targets that could affect HT1's ability to phosphorylate CBC1 for *in vitro* experiments, and our set of experiments builds on that data. To explore both of these topics, *Agrobacterium* vectors were used to make *pGC1:MPK12-GFP/mpk12*, *pGC1:MPK12(K70R)-GFP/mpk12*, *pGC1:CBC1-GFP/cbc1cbc2*, and *pGC1:CBC1(T256A/S280A)-GFP/cbc1cbc2* mutant *A. thaliana* lines that were screened and selected for use in stomatal conductance experiments. The results gathered were compared to the *in vivo* responses gathered from Col-0 (wildtype control accession), *mpk12* mutant plants, and *cbc1/cbc2* double mutant plants. The use of these genetic mutants would determine whether the data that has been observed in in multiple *in vitro* phosphorylation studies have consistent results *in vivo*. Overall, the information gathered from these experiments could be used for developing

mutant lines in agricultural products that can tolerate the increasing atmospheric levels of carbon dioxide we are experiencing as a result of climate change.

## RESULTS

### *1.1 Genotyping and isolation of the *cbc1/cbc2/ht1(A109V)* triple mutant.*

In order to test our hypothesis *in vivo*, a *cbc1/cbc2/ht1(A109V)* triple mutant line had to be constructed. This was achieved by crossing a T-DNA *cbc1/cbc2* double mutant line with an *ht1(A109V)* line. Polymerase chain reaction (PCR) experiments were pursued in the T1 generation to test if the crossing was successful by confirming that the CBC1 and CBC2 genes were heterozygous for each T-DNA insertion with a wildtype allele that originated from the *ht1(A109V)* parent plant. In following generations, samples were first tested to determine whether a sample was homozygous for each of the CBC1 and CBC2 T-DNA insertions before the HT1 gene was amplified via PCR (Fig. 1a-b). DNA samples were then purified and sent in for sequencing to confirm that the A109V point mutation was present and homozygous (Fig. 1c). A successful point mutation would show a nucleotide change of C→T in sequencing with only a single peak, not two peaks overlapping which would indicate that the mutation is heterozygous (Fig. 1d). Samples that met these criteria were selected for use in experiments that would test their stomatal responses to imposed shifts in the atmospheric concentration of carbon dioxide. This *cbc1/cbc2/ht1(A109V)* triple mutant line was compared to WT, *cbc1/cbc2*, and *ht1(A109V)* plants that were all selected for use as controls.

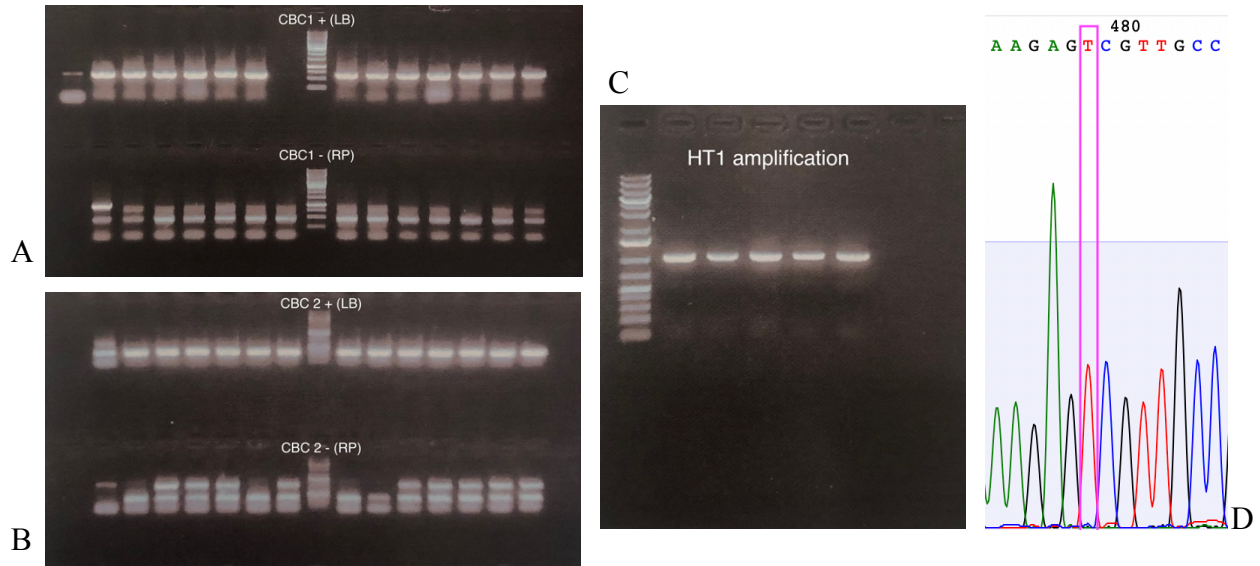


**Figure 1. Polymerase chain reaction and HT1 genetic sequencing used to identify *cbc1/cbc2/ht1(A109V)* triple mutant samples. a-b**, PCR results testing for the presence of T-DNA insertions and homozygosity in each CBC gene (A: *cbc1* and B: *cbc2*). One primer pair was used to test for this insertion, with the results shown in the top row of each gel. In the top row, the presence of a band not seen in the WT sample indicates the presence of the insertion as the LB primer attaches to the left side border of the insertion. Another primer pair was testing for homozygosity of the insertion with the results shown in the bottom row. In the bottom row, having the same bands as the WT sample indicates the lack of insertion because if there were, the distance between the two primers would be too long for the WT band to form. **c**, PCR gel showing results of amplification of the HT1 gene from the genomic DNA of candidates that were sent in for genetic sequencing **d**, Genetic sequencing results showing a successful homozygous point mutation of *ht1(A109V)*.

**Table 1.** PCR primers used for construction of *cbc1/cbc2/ht1(A109V)*.

	Primer Sequence	T <sub>m</sub> (°C)
SALK.LBb1.3	5'-ATTTTGCCGATTTTCGGAAC	52
SAIL_LB1	5'-TAGCATCTGAATTCATAACCAATCTC	58
SALK_005187_LP	5'-ACACCGAAAGAAAGCGAAGAG	55
SALK_005187_RP	5'-TTCGGAAAGAAAGTTTCGATTC	52
SAIL_740_G01_LP	5'-TTTATGCCAAACAGCAACCTC	54
SAIL_740_G01_RP	5'-TCTTTTCCCATTTTCCTCTGC	53
HT1 (A109V check F55)	5'-AACGACGGTTAGATTCTCG	55
HT1 (A109V check R58)	5'-CAAAAGCAAATTGTTGGACTTTAG	58

**Table 2.** Length of expected DNA fragment using primers from Table 1.

	Expected DNA Length (bp)
CBC1 insertion	~650
WT CBC2	1103
CBC2 insertion	~800
WT CBC2	1140
HT1 amplification	1003

## 1.2 Whole leaf gas exchange experiments of the *cbc1/cbc2/ht1(A109V)* triple mutant.

The goal of the experiment was to compare the CO<sub>2</sub> concentration-induced changes in stomatal conductance among the genotypes described above. Stomatal conductance is a measurement of the amount of water vapor that is exiting a leaf through its stomata, of the three different mutants to each other and wildtype (WT). The stomatal conductance phenotype quantitatively reflects the degree of stomatal opening in a plant, higher values indicate a wider stomatal aperture while lower values indicate more narrow apertures. For the experiments, a LiCOR 6400 portable photosynthesis machine automatically changed the concentration of carbon dioxide within the chamber that contained the sample being tested and collected data on changes in stomatal conductance. A program where the concentration of carbon dioxide was shifted from ambient ~400 ppm to high >800 ppm to low <180 ppm was chosen. The WT plants showed normal basal stomatal conductance values of ~0.15 mol H<sub>2</sub>O m<sup>-2</sup>s<sup>-1</sup> when exposed to ambient levels of CO<sub>2</sub> (Fig. 2). In a high CO<sub>2</sub> environment, stomatal conductance values of approximately ~0.10 mol H<sub>2</sub>O m<sup>-2</sup>s<sup>-1</sup> and lower indicate stomatal closure. In environments with low levels of CO<sub>2</sub>, values of ~0.18 mol H<sub>2</sub>O m<sup>-2</sup>s<sup>-1</sup> and higher indicate more open stomata; both of these responses were observed in the WT samples (Fig. 2). The *cbc1/cbc2/ht1(A109V)* triple mutant has both CBC genes knocked out in addition to a mutated HT1 protein that is not deactivated in elevated CO<sub>2</sub>. The triple mutant showed stomatal conductance values similar to the *cbc1/cbc2* double knockout mutant where the stomata remained narrower than WT even when CO<sub>2</sub> levels fluctuated. These results are the opposite of the *ht1(A109V)* single mutant samples that maintained more open stomatal values as a result of the mutated HT1 protein being constantly active. The data from the experiments showed that during carbon dioxide level



fluctuations, the *cbc1/cbc2/ht1(A109V)* triple mutant responded similarly to the *cbc1/cbc2* double mutant as opposed to the *ht1(A109V)* single mutant.

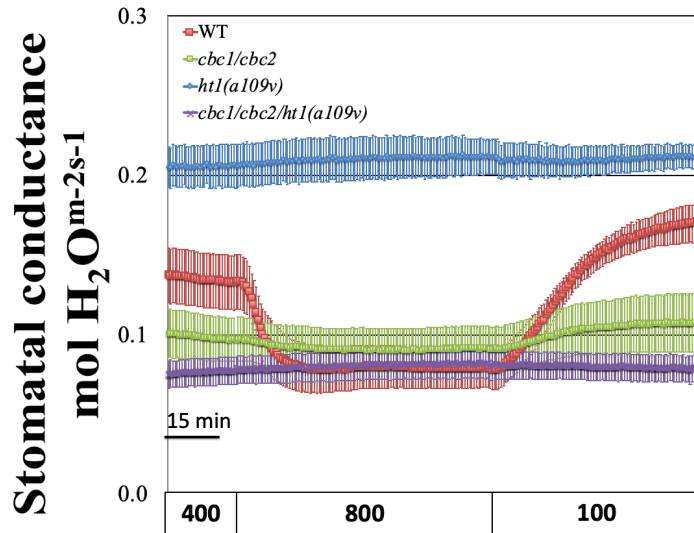


**Figure 2. Stomatal conductance comparisons of Col-0, *cbc1/cbc2*, *ht1(A109V)*, and *cbc1/cbc2/ht1(A109V)*.** The stomatal conductance of samples of *Arabidopsis thaliana* were measured at 400 ppm (parts per million) of CO<sub>2</sub> for 30 minutes, 800 ppm of CO<sub>2</sub> for 60 minutes, and 150 ppm of CO<sub>2</sub> for 50 minutes with a LiCOR 6400 portable photosynthesis system. The average value is represented for genotypes where more than one sample was tested. WT (n=4), *cbc1/cbc2* (n=4), and *ht1(A109V)* (n=4) lines were all used as controls to compare to the *cbc1/cbc2/ht1(A109V)* triple mutant line (n=4).

### 1.3 Construction of MPK12 and CBC1 GFP vectors.

To determine if the 256 and 280 amino acid sites were crucial for the function of CBC1, we decided to transform background *cbc1/cbc2* double mutant plants with two vectors. One vector would have a wildtype CBC1 protein and one vector would express a CBC1 protein with point mutations in two of our hypothesized phosphorylation sites (Fig. 3a). A similar approach was taken to test if kinase activity was required for MPK12 function where a wildtype MPK12 allele and a MPK12 with a K70R point mutation were transformed into *mpk12* background plants via *Agrobacterium* (Fig. 3b). This K70R mutation was in a location where a mutation could impact the kinase activity of MPK12 and therefore its ability to inhibit HT1. A promoter specific to guard cells called *pGCI*, developed in the Schroeder lab, was selected as results have shown strong guard cell expression and therefore was selected to be the promoter for these constructs (Yang et al., 2008). Green fluorescent protein was added to the C-terminal as a tag so that candidates with the vector can be easy to identify using microscopy (Fig. 3a-b). Phusion U Polymerase was used to amplify the genes of interest before USER cloning and Phusion Hot Start II Polymerase was used for amplification before SLiCE cloning, the primers used for both of these cloning reactions are listed in Table 3. Expected lengths of fragments are listed in Table 4 and were used to determine if the cloning was successful before these fragments were transformed into vectors. Additionally, after each cloning step, plasmid purification was done on colonies so that sequencing, done by Retrogen Inc, could confirm that the point mutations were present. The USER cloning allowed for the genes of interest to be placed into a vector with a GFP tag downstream of the gene and the SLiCE cloning was used to place the gene of interest - GFP fragment into a vector with the *pGCI* promoter. The final constructs were vectors that had *pGCI* as its promoter, green fluorescent protein (GFP) downstream of the gene, and contained

the desired WT or mutant CBC1 or MPK12 gene (Fig. 3a-b). Once the final constructs were confirmed via genetic sequencing they were transformed into their respective background plants of *Arabidopsis thaliana* using the *Agrobacterium* transformation method. The vectors that contained an MPK12 gene were transformed into *mpk12* plants while the vectors that contained a CBC1 gene were transformed into *cbc1/cbc2* plants. This was to ensure that the proteins in the plants had the sequence of the gene from the vectors since before the transformation the plants did not have a functioning protein at all. Thousands of seeds were collected and screened on hygromycin plates and samples that germinated were transferred to separate pots and grown in the growth room using a cycle of 16 hours of day with 8 hours of night. When plants were 2-3 weeks old, a sample was taken to determine if the plant did contain the vector with the gene of interest via microscopy. Because there was a GFP tag attached to the end of this gene it made selection of T1 and T2 candidates easy as fluorescence of guard cells were checked using a confocal microscope and compared to wildtype guard cell autofluorescence (Fig. 4a-b).

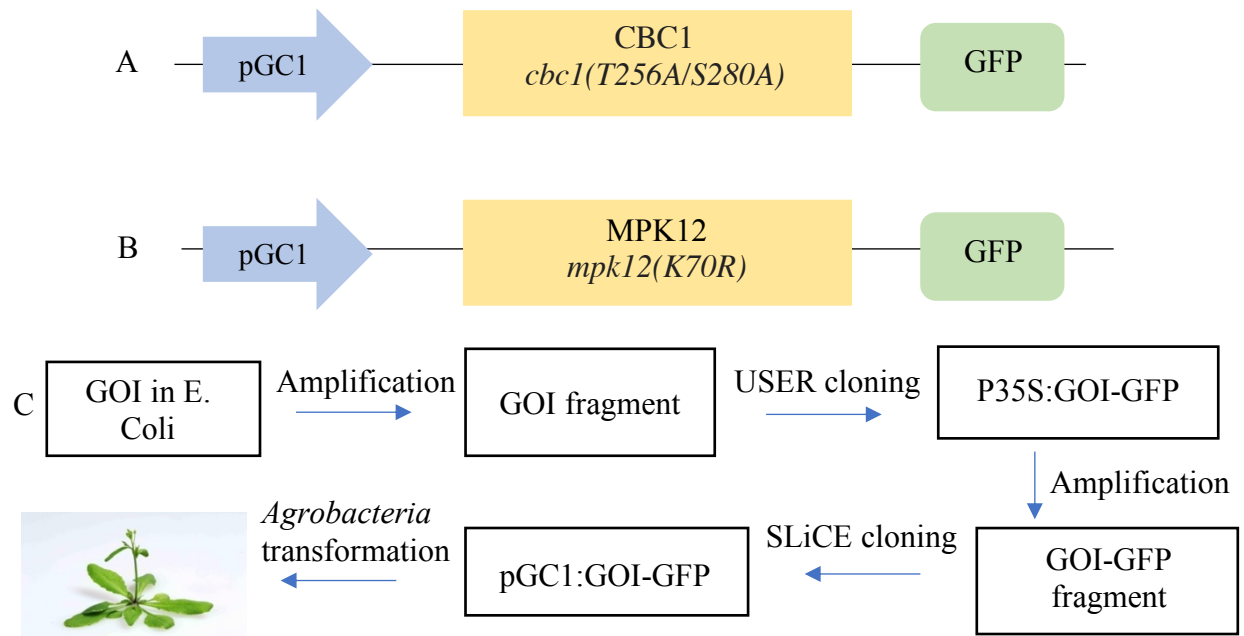


**Figure 3. Construction plan for MPK12 and CBC1 GFP vectors. a-b,** A strong guard cell promoter (*pGC1*) was placed upstream of the gene of interest. Downstream of the gene of interest was green fluorescence protein (*GFP*) that can be used as a marker to determine via confocal microscopy whether samples contain the mutant protein. **c,** a step by step flowchart of how the genes of interest were cloned for the construction of the vectors that were transformed into *A. thaliana* mutant background plants that were mutants for the transforming vector's gene of origin.

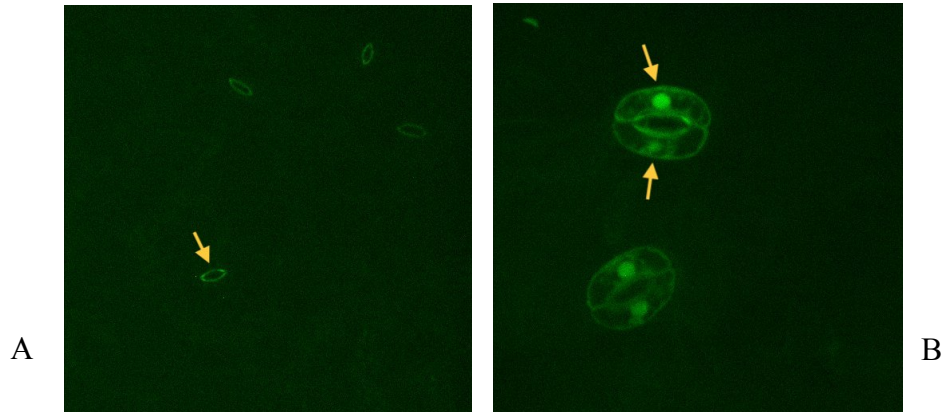


**Figure 4. Confocal results of guard cell GFP fluorescence in a *pGC1:CBC1(T256A/S280A)-GFP/cbc1cbc2* candidate.** These images were taken with a confocal microscope at a magnification of 100x using a GFP filter. **a**, example of stomatal autofluorescence observed in WT samples. **b**, a candidate from one of the *pGC1:CBC1(T256A/S280A)-GFP/cbc1cbc2* lines displaying high fluorescence within the guard cells.

**Table 3.** Primers used for cloning of GFP vectors using USER and SLiCE cloning systems.

	Primer Sequence	T <sub>m</sub> (°C)
CBC1_USER_F55	5'- <b>ggcttaau</b> ATGAAGGAGAAGGCCGGAG	55
CBC1_-stop_USER_R60	5'- <b>ggtttaau</b> TGGGCCTCGGTGTCGG	60
MPK12.user.F54	5'- <b>ggcttaau</b> ATGTCTGGAGAATCAAGCTCTG	54
MPK12.user.R54	5'- <b>ggtttaau</b> GTGGTCAGGATTGAATTTGACAG	54
CBC1_InF_pGC1_F55	5'- <b>aaattctagaggatcc</b> atgAAGGAGA	55
MPK12_InF_pGC1_F54	5'- <b>aaattctagaggatcc</b> ATGTCTGGAGAATCAAGCTC	54
GFP_InF_Nos_R52	5'- <b>cggtacccgggatcc</b> TTATTTGTATAGTTCATCCATGC	52

**Table 4.** Length of expected DNA fragment using primers from Table 3.

	Expected DNA Length (bp)
CBC1 User Cloning	~1200
MPK12 User Cloning	~1200
CBC1 pGC1/Nos	~1900
MPK12 pGC1/Nos	~1900



**Table 5.** Clones, plasmids, and vectors used from or added to the Julian Schroeder's lab stocks.

Ref #	Stock Type	Clone Name	General Description	Vector	Strain	Antibiotic
3949	DNA Box #41	pGEX-6P1-user	USER compatible E. coli overexpression vector	pGEX-6P1-user	N/A	Carbenicillin
4551	DNA Box #58	pGEX-4T-1-MPK12	wide-type MPK12	N/A	N/A	N/A
4554	DNA Box #58	pGEX-4T-1-MPK12-K70R	Kinase-inactive MPK12(K70R)	N/A	N/A	N/A
5502	Glycerol Stock Box #70	pGEX6P-CBC1	CBC1 protein expression	pGEX6P-1user	BL21	Ampicillin
5953	DNA Box #75	GST-CBC1-T256/S280A	E. Coli Expression vector	pGEX-6P-1	N/A	Carbenicillin
5969	DNA Box #75	pGC1:CBC1-GFP	Stable Expression vector	pCAMBIA1300	N/A	Kanamycin/Hygromycin
5970	DNA Box #75	pGC1:CBC1(T256/S280A)-GFP	Stable Expression vector	pCAMBIA1300	N/A	Kanamycin/Hygromycin
5971	DNA Box #75	pGC1:MPK12-GFP	Stable Expression vector	pCAMBIA1300	N/A	Kanamycin/Hygromycin
5972	DNA Box #75	pGC1:MPK12(K70R)-GFP	Stable Expression vector	pCAMBIA1300	N/A	Kanamycin/Hygromycin
5922	DNA Box #75	35S:user-GFP	Protoplast Transient Expression vector	pUC18	N/A	Carbenicillin

*1.4 Whole leaf gas exchange experiments of pGC1:CBC1(T256A/S280A)-GFP/cbc1cbc2 and pGC1:CBC1-GFP/cbc1cbc2 mutant lines.*

As expected, the WT stomata became narrower when carbon dioxide levels increased and more open when the CO<sub>2</sub> levels decreased (Fig. 5). The *cbc1/cbc2* double mutant does not have functioning CBC1 or CBC2 proteins and these samples showed low levels of stomatal conductance  $\sim 0.085 \text{ mol H}_2\text{O m}^{-2}\text{s}^{-1}$  and displayed no clear response to an increase in CO<sub>2</sub> levels and a small increase in stomatal conductance (to  $\sim 0.10 \text{ mol H}_2\text{O m}^{-2}\text{s}^{-1}$ ) when the CO<sub>2</sub> concentration changed to 100 ppm (Fig. 6). Samples from the *pGC1:CBC1-GFP/cbc1cbc2* have a WT CBC1 protein but no functioning CBC2 protein. These samples had responses to carbon dioxide shifts that were more comparable to the WT samples with a basal stomatal conductance that was slightly elevated ( $\sim 0.16 \text{ mol H}_2\text{O m}^{-2}\text{s}^{-1}$ ) (Fig. 5). The other mutant line, *pGC1:CBC1(T256A/S280A)-GFP/cbc1cbc2*, has a nonfunctional CBC2 protein and a CBC1 protein with two point mutations at potential phosphorylation sites. These samples exhibited low stomatal conductance levels that did not change dramatically when CO<sub>2</sub> levels increased to 800 ppm and only increased slightly when CO<sub>2</sub> levels decreased, similar to the *cbc1/cbc2* mutant results (Fig. 5). The results from the experiments show that the WT and *pGC1:CBC1-GFP/cbc1cbc2* plants both had similar responses to changes in CO<sub>2</sub> concentrations by having narrower stomata when carbon dioxide levels are high and more open stomata when carbon dioxide levels are low. Conversely, both the *cbc1/cbc2* and *pGC1:CBC1(T256A/S280A)-GFP/cbc1cbc2* samples showed overall trends of low stomatal conductance levels that did not indicate acclimation to fluctuations in carbon dioxide levels.

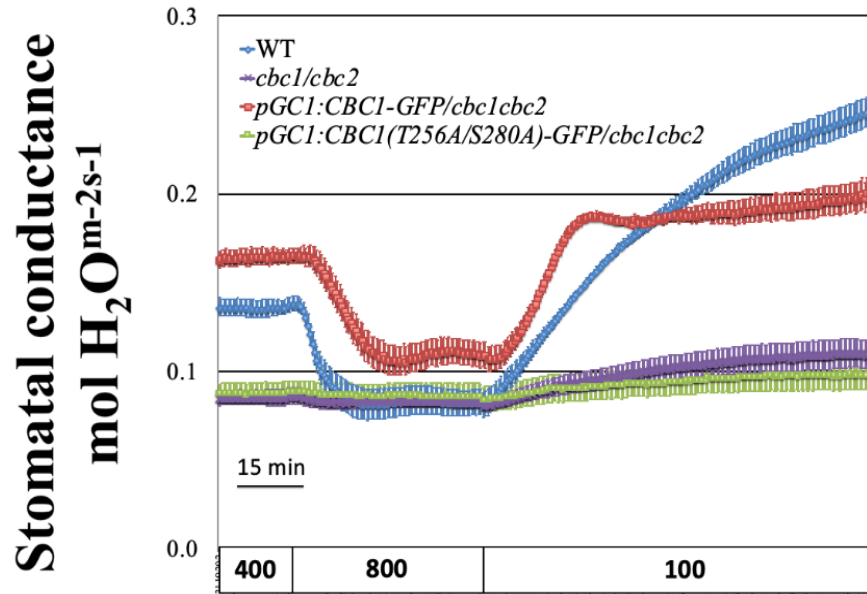


**Figure 5. Stomatal conductance comparisons of WT, *cbc1/cbc2*, *pGC1:CBC1(T256A/S280A)-GFP/cbc1cbc2* and *pGC1:CBC1-GFP/cbc1cbc2*.** The stomatal conductance of samples of *Arabidopsis thaliana* were measured at 400 ppm of CO<sub>2</sub> for 30 minutes, 800 ppm of CO<sub>2</sub> for 45 minutes, and 150 ppm of CO<sub>2</sub> for 90 minutes with a LiCOR 6400-XT portable photosynthesis system. The average value is represented for genotypes where more than one sample was tested. WT (n=4) and *mpk12* (n=4) lines were used as controls and compared to the *pGC1:CBC1-GFP/cbc1cbc2* (n=4) and *pGC1:CBC1(T256A/S280A)-GFP/cbc1cbc2* (n=4) mutant lines.

1.5 Whole leaf gas exchange experiments of *pGCI:MPK12-GFP/mpk12* and *pGCI:MPK12(K70R)-GFP/mpk12* mutant lines.

The goal for this set of experiments was to determine whether kinase activity was required for MPK12 function in the carbon dioxide signaling pathway by exposing different genotype samples to changing atmospheric carbon dioxide concentrations and observing their stomatal responses. The results for the WT control samples showed stomatal closure in high carbon dioxide concentrations and more open stomata under low carbon dioxide concentrations as expected (Fig. 6). The *mpk12* control samples do not have a functioning MPK12 protein and showed an elevated stomatal resting state compared to WT ( $\sim 0.24$  vs.  $\sim 0.13$  mol H<sub>2</sub>O m<sup>-2</sup>s<sup>-1</sup>) and remained elevated during the shifts in atmospheric CO<sub>2</sub> levels which is consistent with other academic literature (Fig. 6). The *pGCI:MPK12-GFP/mpk12* samples are *mpk12* plants that have a WT MPK12 allele and so should exhibit a rescue phenotype that looks similar to the WT results. In this experiment, these plants had lower levels of stomatal conductance when exposed to higher levels of CO<sub>2</sub> and higher stomatal conductance when CO<sub>2</sub> levels decreased, an overall response that was similar to our WT controls (Fig. 6). The *pGCI:MPK12(K70R)-GFP/mpk12* plants were *mpk12* plants that were transformed with an MPK12 protein that has a K70R amino acid mutation that prevents kinase activity since the ATP-binding site was mutated. The plant samples that expressed kinase inactive MPK12, showed stomatal responses that were similar to both WT and *pGCI:MPK12-GFP/mpk12* as the stomatal conductance increased with low levels of CO<sub>2</sub> and decreased in response to higher CO<sub>2</sub> concentrations (Fig. 6). The data from this experiment showed that the samples from the *pGCI:MPK12-GFP/mpk12* and *pGCI:MPK12(K70R)-GFP/mpk12* mutant lines had similar responses to the WT samples in

relation to their basal stomatal conductance levels and stomatal responses to changes in atmospheric carbon dioxide levels.

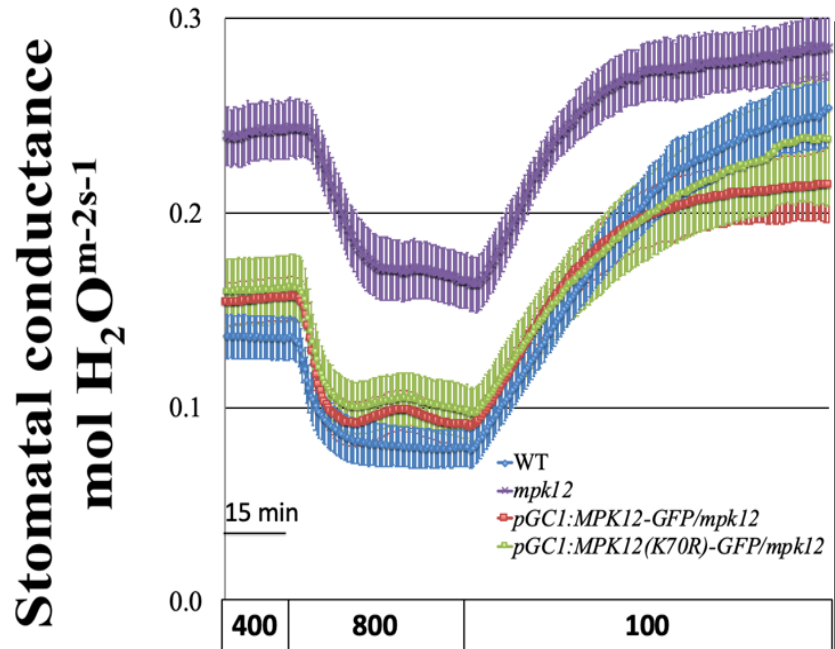


**Figure 6. Stomatal conductance comparisons of WT, *mpk12*, *pGC1:MPK12-GFP/mpk12* and *pGC1:MPK12(K70R)-GFP/mpk12*.** The stomatal conductance of samples of *Arabidopsis thaliana* were measured at 400 ppm of CO<sub>2</sub> for 30 minutes, 800 ppm of CO<sub>2</sub> for 45 minutes, and 150 ppm of CO<sub>2</sub> for 90 minutes with a LiCOR 6400-XT portable photosynthesis system. The average value is represented for genotypes, where more than one sample was tested. WT (n=6) and *mpk12* (n=5) lines were used as controls and compared to the *pGC1:MPK12-GFP/mpk12* (n=6) and *pGC1:MPK12(K70R)-GFP/mpk12* (n=6) mutant lines.

## DISCUSSION

### *cbc1/cbc2/ht1(A109V)*

Previous research has shown that in *Arabidopsis thaliana* and in other C3 and C4 land plants, fluctuations in atmospheric levels of carbon dioxide affect the stomatal conductance levels due to changes in the width of the stomatal aperture. Recent research has suggested that the early CO<sub>2</sub> signaling pathway is not directly mediated by the signaling pathway triggered by the plant stress hormone abscisic acid (Hsu et al., 2018). Additionally, HT1, a protein kinase present within the carbon dioxide signaling pathway was shown to have the ability to phosphorylate both wildtype and kinase dead CBC1/CBC2 proteins *in vitro* (Hiyama et al., 2017). However, the effect or *in vivo* relevance of this CBC1 phosphorylation has remained unknown. Separate *in vitro* experiments indicated that phosphorylation of CBC1 by HT1 was inhibited by MAP kinase proteins MPK4 and MPK12 when bicarbonate was present (Y. Takahashi, Unpublished). Taking these results into account, a hypothesis that CBC1/CBC2 are epistatic to HT1 in the carbon dioxide signaling pathway was developed and one goal of this study was to test this theory *in vivo* using genetic mutants.

The goal for this set of experiments was to determine if the CBC1/CBC2 proteins operated in the carbon dioxide-induced signal transduction pathway, specifically downstream of HT1, by comparing the stomatal conductance phenotypes of mutants that had different activity levels of HT1, CBC1, and CBC2. Current hypotheses for models of this pathway are based on previous yeast two-hybrid and phosphorylation assay experiments that suggested that the proteins MPK4/MPK12 are able to interact and inhibit HT1 activity (Jakobson et al., 2016). The genetically dominant HT1 point mutation A109V was chosen because previous experiments

have shown that this mutation allows for stomata to remain open and stomatal conductance levels are elevated (Hörak et al., 2016) (; Y. Takahashi et al., unpublished).

Our experimental data showed that despite the *cbc1/cbc2/ht1(A109V)* triple mutant being exposed to varying levels of atmospheric carbon dioxide, the stomatal conductance remained low and had responses similar to the *cbc1/cbc2* samples (Fig. 2). In contrast, the *ht1(A109V)* samples retained elevated stomatal conductance levels when compared to Col-0 (WT control) samples and showed minimal fluctuations despite the changes in carbon dioxide levels (Fig. 2). The general trend for Col-0 control samples in similar experiments is that stomatal apertures close and stomatal conductance levels decrease when exposed to elevated carbon dioxide levels while in environments with low levels of carbon dioxide, the stomatal apertures will open and accommodate an increase in stomatal conductance levels (Hsu et al., 2018). The Col-0 samples used in these experiments showed results consistent with these trends (Fig. 2).

Although the triple mutant contained the A109V point mutation in its HT1 gene which would render HT1 unable to be inhibited by MPK4/MPK12 (Y. Takahashi et al., unpublished), the *cbc1/cbc2/ht1(A109V)* triple mutant did not show a similar response to the *ht1(109V)* single mutant (Fig. 2.). Our working hypothesis was the CBC1/CBC2 kinases act downstream of HT1 and that HT1 phosphorylates CBC1/CBC2 which contributes to keeping stomatal apertures open. Seeing as the A109V point mutation in the HT1 protein inhibits MPK4/MPK12's ability to deactivate HT1 (Y. Takahashi et al., unpublished), we would expect that samples with this mutation would exhibit elevated stomatal conductance levels (Hörak et al., 2016). The *cbc1/cbc2/ht1(A109V)* triple mutant line has a perpetually active HT1 protein and knocked out CBC1 and CBC2 genes. Whether the samples of this mutant line will exhibit stomatal response phenotypes similar to the *ht1(A109V)* samples would be dependent on whether CBC1/CBC2 is



epistatic to HT1 in the signal transduction pathway. If changes in the width of the stomatal aperture are not dependent on phosphorylation/dephosphorylation of CBC1/CBC2 by HT1 then we would expect that the *cbc1/cbc2/ht1(A109V)* triple mutant would have a similar open stomatal phenotype to the *ht1(A109V)* mutant. This is because in theory, there would be no mutated proteins downstream of the constantly active *ht1(A109V)* protein that would trigger the closure of the stomata. However, the triple mutant samples had similar stomatal conductance responses to changes in carbon dioxide levels when compared to the *cbc1/cbc2* mutants (Fig. 2.). This suggests that CBC1/CBC2 are present in the carbon dioxide signal transduction pathway and function downstream of HT1. For future experiments, I would like to take infrared thermal images of the four genotypes used in these experiments to determine whether there is a difference in leaf temperature due to the varying stomatal responses of each genotype. I think it would be helpful to investigate whether the activity levels of the CBC1/CBC2 proteins significantly change a plant's leaf temperature seeing as having more narrow stomata results in higher leaf temperatures while more open stomata result in lower leaf temperatures (Brown and Escombe, 1905; Huber, 1935; Raschke 1960; Jackson 1982, as cited by Jones, 2004).

It is possible that there are additional undiscovered protein(s) involved in this carbon dioxide-induced signal transduction pathway. These potential protein(s) could be located downstream of HT1 but upstream of CBC1/CBC2. It is also conceivable that these two proteins do not interact directly with each other *in vivo*. Our observed results would not change if this is the case because the phenotypes in this experiment were dependent solely on the existence of CBC1/CBC2 in the pathway, not on if CBC1/CBC2 is interacting directly with HT1. Seeing that recent research has shown *in vitro* protein interactions between HT1 and CBC1 there will need to be future experiments to confirm whether HT1 and CBC1/CBC2 directly interact *in vivo* or if

there are other possible protein(s) involved (Y. Takahashi et al., unpublished). Some approaches that could be used to observe such protein interactions *in vivo* are fluorescence resonance energy transfer (FRET) microscopy or bimolecular fluorescence complementation (BiFC) as both procedures emit defined fluorescent signals when the involved proteins have close interactions.

### ***MPK12 GFP Vectors***

A known component in the beginning of the carbon dioxide signaling pathway are the mitogen-activated protein kinases (MAPK), in *A. thaliana* there is MPK4 and MPK12. This was suggested by a set of experiments that used mutants where a guard cell specific promoter that suppresses MPK4 was transformed into background *mpk12* plants to form a double mutant line (Töldsepp et al., 2018). Using samples from two independent *mpk12 mpk4GC* lines this study observed normal stomatal responses when exposed to the plant stress hormone abscisic acid (ABA) but elevated stomatal conductance levels that did not fluctuate despite the atmospheric levels of carbon dioxide changing (Töldsepp et al., 2018). A separate study also found that MPK4 and MPK12 have the ability to inhibit HT1 phosphorylation activity *in vitro* (Höřak et al., 2016). A separate study found that an MPK12 protein with a K70R point mutation designed to remove the protein's kinase activity retained its ability to inhibit both HT1's ability to autophosphorylate and to phosphorylate other proteins, in that case, casein (Jakobson et al., 2016). Finally, recent *in vitro* phosphorylation assays with MPK12-K70R, CBC1, and HT1 showed consistent results where CBC1 phosphorylation by HT1 still occurred, but this phosphorylation is inhibited when bicarbonate is added suggesting that the presence of bicarbonate indirectly inhibits CBC1 phosphorylation (Y. Takahashi et al., unpublished). It's possible the presence of the bicarbonate affects the binding activity of MPK4/MPK12 to HT1

and therefore prevents HT1 phosphorylation of CBC1 as *in vitro* pull-down assays showed that in the presence of bicarbonate, HT1 and MPK4 bind together more strongly (Y. Takahashi et al., unpublished). However, other experiments have shown that the protein kinase activity of MPK4 acts independently from MPK12 and was not directly affected *in vitro* by the presence of bicarbonate. This suggests that there could be an additional component upstream of the MPK proteins (Töldsepp et al., 2018).

The goal for this set of experiments was to determine if kinase activity of MPK12 was required for MPK12 function *in vivo* by constructing genetic mutants and comparing their stomatal conductance responses. For this purpose, a vector containing the K70R point mutation was chosen when constructing the *Agrobacteria* vector that would be used in conjunction with a guard cell specific promoter (*pGCI*) and a green fluorescent protein (*GFP*) tag (Fig. 3a-b). These vectors were transformed into samples of a T-DNA *mpk12* line that has the MPK12 gene knocked out to ensure that if there were MPK12 proteins functioning in these transformed samples, they would be the result of a successful insertion by the vector (Fig. 3a-b). Samples used in stomatal conductance experiments were selected based on whether strong GFP fluorescence was visible within the guard cells of stomata indicating that the vector with the desired gene of interest, was present in the genome of that sample (Fig. 4). Samples from three independent *pGCI:MPK12(K70R)-GFP/mpk12* mutant lines and four independent *pGCI:MPK12-GFP/mpk12* were used for the stomatal conductance experiments in plants with intact leaves attached to live plants. The results were compared to responses observed in samples of Col-0 (WT) controls and the single *mpk12* T-DNA insertion mutant (Fig. 6).

The Col-0 control samples used in these experiments were consistent with general WT trends where we observed lower stomatal conductance values as the carbon dioxide

concentration increased followed by higher levels of stomatal conduction when the carbon dioxide concentration decreased (Fig. 6) (Hsu et al., 2018). The *mpk12* samples showed an elevated level of steady state stomatal conductance when compared to Col-0 ( $\sim 0.242 \text{ mol H}_2\text{O m}^{-2}\text{s}^{-1}$  vs  $\sim 0.135 \text{ mol H}_2\text{O m}^{-2}\text{s}^{-1}$ ) and while these samples did show stomatal responses that would increase and decrease in response to the fluctuating carbon dioxide levels, the samples maintained an overall elevated stomatal conductance (Fig. 6). These data are consistent with previous experiments that showed similar results in three lines that had different mutations within the MPK12 gene that affected the MPK12 protein's ability to function (Jakobson et al., 2016). Note that *mpk12/mpk4* double mutants are needed to more strongly disrupt the CO<sub>2</sub> response (Töldsepp et al., 2018). However, this double mutant already uses the pGC1 promoter to silence *MPK4* in guard cells (Töldsepp et al., 2018), making this promoter less suitable for our MPK12 complementation experiments.

The *pGC1:MPK12-GFP/mpk12* mutant line was constructed for the purpose of acting similar to a control as this control vector contains a wildtype MPK12 cDNA so that if transformation was successful, the samples would show a rescue phenotype when used in the stomatal conductance analysis experiments. These MPK12 rescue samples should show similar stomatal responses to the Col-0 controls since the *mpk12* background plant would have received a working MPK12 gene from the *Agrobacterium* vector (Fig. 3b). The samples from four independent *pGC1:MPK12-GFP/mpk12* lines had similar steady state stomatal conductance levels and responses to changes in the concentration carbon dioxide when compared to Col-0, exhibiting a rescue phenotype (Fig. 6). The *pGC1:MPK12(K70R)-GFP/mpk12* samples whose MPK12 proteins contained the point mutation that would remove MPK12's kinase activity had similar steady state stomatal conductances and stomatal responses to fluctuations in carbon

dioxide to the Col-0 control samples (Fig. 6). These results suggest that the ability of MPK12 to inhibit HT1 activity was not impeded by the loss of its kinase activity.

It is possible that there is(are) some kind of additional element(s) operating upstream of the MPK4/MPK12 proteins as the protein kinase activities of MPK12 and MPK4 were not directly affected by the presence of bicarbonate *in vitro* (Töldsepp et al., 2018). While the presence of bicarbonate does stabilize the binding between MPK4 and HT1 (Y. Takahashi et al., unpublished) it is unknown whether we would see similar results *in vivo*. Procedures like BiFC and FRET microscopy would be viable options as these procedures can be used to observe *in vivo* protein interactions. Steps to see if there are additional components operating upstream of MPK4/12 that are currently unknown would take some time but could be done by performing a forward genetic screen.

### ***CBC1 GFP Vectors***

In recent years, there has been the identification of a new component in the carbon dioxide signal transduction pathway that functions upstream of the slow anion channel-associated 1 (SLAC1) protein responsible for fluctuations in ion concentration within the guard cells of stomata by affecting the turgor pressure and overall aperture width. These two new kinase proteins were named convergence of blue light and CO<sub>2</sub> (CBC) 1 and 2 (Hiyama et al., 2017). Single mutant lines and a double mutant line were developed to determine how these proteins contributed to responses to changes in carbon dioxide concentrations. The *cbc1* and *cbc2* lines showed only weak stomatal opening responses as the carbon dioxide levels were lowered experimentally, but the samples were stunted and only reached  $\sim 0.6 \text{ mol H}_2\text{O m}^{-2}\text{s}^{-1}$  compared to the Col-0 wildtype control samples that reached as high as  $\sim 0.11 \text{ mol H}_2\text{O m}^{-2}\text{s}^{-1}$

(Hiyama et al., 2017). The *cbc1/cbc2* line showed no noticeable fluctuations in its stomatal conductance levels and remained around  $\sim 0.3 \text{ mol H}_2\text{O m}^{-2}\text{s}^{-1}$  for the entirety of the experiment despite the carbon dioxide levels decreasing multiple times before returning to ambient levels (Hiyama et al., 2017). These results might be explained by a model in which CBC1 and CBC2 were present in the carbon dioxide signaling pathway and this same study also found that CBC1/CBC2 had autophosphorylation activity and that HT1 had the ability to phosphorylate kinase-dead CBC1 and CBC2 *in vitro* but that CBC1/CBC2 could not phosphorylate HT1 (Hiyama et al., 2017). The effect and relevance of HT1-mediated phosphorylation of CBCs remained however unknown.

The goal of the experiments was to identify potential HT1-mediated phosphorylation sites in CBC1 that might be important in the carbon dioxide signaling pathway *in vivo* by comparing the stomatal response in specially designed mutants to those of Col-0 and *cbc1/cbc2*. To determine a list of potential phosphorylation site targets for HT1 on the CBC1 protein that we could target, data from a mass spectrometry experiment performed on *in vitro* phosphorylation assays of wildtype and mutant inactive CBC1 protein with and without the presence of HT1 was used as a reference (Y. Takahashi et al., unpublished). The mass spectrometry experiments identified eight possible phosphorylation sites across the CBC1 protein and by comparing the results to the data collected from the kinase inactive CBC1 protein experiment, the amino acid sites of Thr-256 and Ser-280 were chosen as mutation targets as both are located near the activation loop of CBC 1 (Y. Takahashi et al., unpublished). There were two *Agrobacterium* vector lines constructed for this set of experiments, the first contained a wildtype copy of the CBC1 gene while the other contained both of the previously mentioned CBC1 point mutations (Fig. 3a). Both of these CBC1 gene constructs were placed into a vector with a guard cell

preferential *pGCI* promoter (Yang et al., 2008) to ensure expression in guard cells and a *GFP* protein at the C-terminus to ensure that there would be an observable tag that could be used for screening samples (Fig. 3a). These vectors, with their respective genes of interest, were transformed into *cbc1/cbc2* double mutant plants and samples were selected for stomatal response experiments only if the samples exhibited strong *GFP* fluorescence within the guard cells of the stomata outside of the general autofluorescence observed in the stomata of Col-0 which so as to indicate the presence of our *GFP* vector within the genome of the candidate sample (Fig. 4a-b). The presence of these vectors indicated that these plants, whose parent had no functional *CBC1* gene, now contained either a wildtype or double mutant *CBC1* gene that was inserted into the genome by their respective *Agrobacterium* vectors.

The two controls used in these experiments were Col-0 (WT) and *cbc1/cbc2*, the Col-0 samples had the expected responses of a decreasing stomatal conductance when carbon dioxide levels went from 400ppm to 800ppm followed by increased stomatal conductance when the carbon dioxide concentration shifted from 800ppm to 100ppm (Fig. 5). Consistent with previous research, the samples from the *cbc1/cbc2* line showed low stomatal conductance levels around  $0.1 \text{ mol H}_2\text{O m}^{-2}\text{s}^{-1}$  that did not fluctuate substantially when carbon dioxide levels rose while stomatal conductance levels rose slightly when the carbon dioxide levels became low (Fig. 5) (Hiyama et al., 2017).

The *pGCI:CBC1-GFP/cbc1cbc2* lines contain a wildtype copy of the *CBC1* gene and if the transformation was successful, we would expect to observe some kind of rescue phenotype that would restore the sample's ability to respond to fluctuations in carbon dioxide levels. The samples of the *pGCI:CBC1-GFP/cbc1cbc2* line that were used showed a higher steady stomatal conductance when compared to Col-0 ( $\sim 0.16 \text{ mol H}_2\text{O m}^{-2}\text{s}^{-1}$  vs  $\sim 0.13 \text{ mol H}_2\text{O m}^{-2}\text{s}^{-1}$ ) and also

displayed more narrow stomata in high carbon dioxide and stomata opening in low carbon dioxide environment although once the conductance levels reached  $\sim 0.195 \text{ H}_2\text{O m}^{-2}\text{s}^{-1}$ , the conductance plateaued while the stomatal conductance of Col-0 samples continued to increase as the carbon dioxide levels remained at 100ppm (Fig. 5). The *pGCI:CBC1(T256A/S280A)-GFP/cbc1cbc2* lines contained a CBC1 gene with the two point mutations T256A and S280A that were selected based on the previously mentioned mass spectrometry data. These samples had a steady stomatal conductance comparable to the *cbc1/cbc2* mutants ( $\sim 0.87 \text{ mol H}_2\text{O m}^{-2}\text{s}^{-1}$  vs  $\sim 0.84 \text{ mol H}_2\text{O m}^{-2}\text{s}^{-1}$ ) and showed similar stomatal responses with the only change being a slight increase after the carbon dioxide levels decreased to 100ppm (Fig 5.) These results suggest that these two possible HT1-specific phosphorylation sites could be crucial for CBC1 activation by HT1 seeing as the mutation of these sites resulted in a phenotype similar to plants that contained no functioning CBC1 protein.

While previous experiments support the hypothesis that HT1 and CBC1 interact, it remains unconfirmed whether HT1 and CBC1 interact via direct binding interactions *in vitro* or *in vivo*. For future experiments, would be interesting to use the information gathered in these experiments to test if there are direct interactions between HT1 and CBC1. One possible approach to determine this could include pull-down assays using wildtype CBC1 and *cbc1(T356A/S280A)* to confirm first *in vitro* that there are physical interactions between these two proteins. Follow up experiments could involve using procedures such as FRET microscopy or BiFC to determine if there are direct interactions *in vivo*. Learning as much information as possible about the interactions and phosphorylation sites of proteins present in the signal transduction pathway for carbon dioxide signaling is crucial for the future of the food supply of the world. The information identified from these studies will be useful in determining potential



target genes and specific amino acid mutations that can be of use in the development of genetically modified agricultural products that will be less vulnerable to the changes in the atmospheric levels of carbon dioxide caused by climate change.

Material in this thesis has been submitted for publication of the material as it may appear in *Science Advances*, 2022, Bosmans, Krystal; Yohei Takahashi., Po-Kai Hsu, Karnelia Paul, Chung-Yueh Yeh, Yuh-Shuh Wang, Dmitry Yarmolinsky, Maija Sierla, Triin Vahisalu, Jaakko Kangasjarvi, Hannes Kollist, Li Zhang, Thien Trac, and Julian I. Schroeder. The thesis author was the primary investigator and author of this paper.

## MATERIAL AND METHODS

### *1.1 Plant growth conditions.*

*Arabidopsis thaliana* seeds were put into a microcentrifuge tube and a solution of 800 $\mu$ L milli-q water, 200 $\mu$ L bleach, and 5 $\mu$ L of 20% Triton X-100 was made. The tube was shaken until bubbles were visible and left to sit for 15 minutes. The tube was put in a mini centrifuge for ~30 seconds and the supernatant was removed. 1 mL of milli-q water was added to the tube to act as a wash and the contents were shaken before being centrifuged again for ~30 seconds followed by removing the supernatant. This wash step was done twice. In a hood under sterile conditions, ~100 $\mu$ L of 0.05% agar was added to the tube to suspend the seeds. Individual seeds were then placed on a ½ Murashige and Skooge (Sigma) plate that had a pH of 5.7/5.8. The plate was then placed in a 4°C environment for 3 days before being placed into a growth room with 16 hours of day and 8 hours of night conditions, if the samples were grown for use in gas exchange experiments then the plates were placed into a plant growth chamber (AR-41L2; Percival Scientific, Perry, Iowa, USA). The settings on the growth chamber were 12 hours of light and 12 hours of dark with ~111  $\mu$ mol m<sup>-2</sup> s<sup>-1</sup> light, CO<sub>2</sub> levels ~600 p.p.m., 55-65% relative humidity, and a temperature of 21°C. After 7-10 days, germinated seedlings were transferred to individual small pots with sterilized soil for continued growth.

### *1.2 Hygromycin Selection Assays.*

Approximately 80mg of seeds (1,000-1,500 seeds) were put into a microcentrifuge tube along with 1mL of 70% ethanol and 5 $\mu$ L of 10% SDS. The tube was shaken to allow for mixing and the contents were left to incubate for 20 minutes. The contents were spun down for ~30 seconds using a minicentrifuge and the supernatant was removed. The contents were washed using 1mL of 100% ethanol, spun down, and the supernatant removed. This ethanol washing step was done twice. The tube was then placed in a sterilized environment inside a hood for 60-90 minutes to allow the seeds to dry out. The seeds were then spread onto selection plates, the plates used were ½ Murashige and Skooge (Sigma) with 100  $\mu$ g/mL hygromycin. The plates were wrapped in aluminum foil and left in a 4°C environment for 3 days before being moved into the growth room with growing conditions of 16 hours of day and 8 hours of night. After 7-10 days seedlings that had germinated were transferred into individual small pots filled with sterilized soil to allow for further growth.

### *1.3 Genome extraction from plants.*

When samples were 2-3 weeks old, one or two small leaves were cut from the parent plant and placed into a labeled microfuge tube. 50 $\mu$ L of an autoclaved DNA extraction buffer made of 100mL of 1M Tris-HCl (pH 7.5), 25mL of 5M NaCl, 25mL of 0.5M EDTA Disodium (pH 8.0), 25mL of 10% SDS, and 325mL of double distilled water (ddH<sub>2</sub>O) was added to the microfuge tube and a disposable pestle was used to lightly grind the leaves. An additional 150 $\mu$ L of the DNA extraction buffer was added to the tube and the leaves were grinded even further using the pestle until there were no visible pieces left. The pestle was sterilized with 100% ethanol before being used to grind each sample. The tube was centrifuged at 14,500 rotations per minute (RPM) for five minutes, during this time 150 $\mu$ L of 100% 2-propanol was added to a new microcentrifuge tube. When the sample was ready, 150 $\mu$ L of the grinded sample was added to the tube with the 2-propanol and homogenized. Samples were placed in a -20 °C freezer for ~15 minutes then centrifuged at 4°C with a speed of 12,000 RPM for 15 minutes. Upon removal from the centrifuge, all of the supernatant was removed and 50 $\mu$ L of milli-q water was added to the tube with the genomic DNA and placed on a Vortex Genie 2 (Fisher) for a couple of seconds to ensure that the water reached all areas where genomic DNA material could be concentrated. Samples were then stored in a -20 °C freezer until they were needed.

#### *1.4 Crossing Arabidopsis thaliana samples.*

Plants were placed in medium sized pots with four seedlings in each one and grown in an open growth room that was kept at 70 °F with a light cycle of 16 hours of day and 8 hours of night until samples were flowering. Samples used for crossing included *cbc1/cbc2* and *ht1(A109V)* and all parent plants were confirmed via PCR to be the correct genotype before being used in crossing. To start, a flower bud on one parent plant that had not bloomed yet would be taken apart using tweezers until only the pistil remained. Then, on a parent plant of the other genotype, a blooming flower would have all parts removed until the stamen with the pollen could be removed. Several stamens would then be tapped onto the pistil from the first parent plant so that the pollen could enter the pistil and fertilize the plant. After each fertilization event was done, a small colored thread was tied around the branch so that artificially fertilized pistils could be easily located later. This process would be repeated until every parent plant had 5-7 fertilization sites and were then returned to the growth room. After ~2 weeks of continued growth, successful fertilization attempts will have produced seeds that were harvested and used a starting point for the isolation of higher order mutants in the next generation.

### 1.5 *E. coli* transformation.

To begin, competent *E. coli* cells were removed from a -80°C freezer and put on ice for two minutes. After these two minutes the reaction product containing the genomic product intended to be inserted into the *E. coli* was added to the cells and continued to be incubated on ice for an additional 30 minutes. During these 30 minutes, 500µL of lysogeny broth (LB) medium was placed in a microfuge tube and incubated at 37°C. After the 30 minutes of incubation, the microfuge tube with the cells and product were incubated at 42°C for 50 seconds before the 500µL of 37°C LB medium was added. This mixture was then placed on a shaker inside a room heated to 37°C for one hour. The cells were then taken to a hood so that they could be spread over an LB plate with 100µg/mL of whatever antibiotic the plasmid had resistance for in a sterile environment. Once the LB medium containing the *E. coli* cells had dried on the plate, it was taken back to the 37°C room overnight before the plate was checked for any colony growth the following morning.

### 1.6 Cloning of MPK12 and CBC vectors.

To mutate an MPK12 gene to contain the *K70R* point mutation, mutagenesis was performed. A reaction of 6.6 $\mu$ L of milli-q water, 1 $\mu$ L of 10x pfu Turbo buffer (Agilent), 1 $\mu$ L of 2.5mM dNTPs, 0.5 $\mu$ L of an *mpk12* plasmid, 0.3 $\mu$ L of MPK12\_K70R\_Fw primer, 0.3 $\mu$ L of MPK12\_K70R\_Rv primer, and 0.3 $\mu$ L of PfuTurbo DNA Polymerase (Agilent) was made (Table 3). After the solution was made, 0.5 $\mu$ L of the restriction enzyme DpnI (New England BioLabs) was added to the reaction and incubated at 37 $^{\circ}$ C for 90 minutes. After incubation, the reaction product was used in the transformation of the JM109 *E. coli* strain and plated on a lysogeny broth (LB) plate that contained 100 $\mu$ g/mL of Kanamycin. The plate was left overnight at 37 $^{\circ}$ C and colonies were purified using a GeneJET Plasmid Miniprep Kit (Thermo Scientific). Plasmids that contained the WT and mutated genes of interest (GOI) were amplified using forward and reverse primers specific to the genes of interest and their intended use in USER cloning (Table 3). Each reaction contained 28 $\mu$ L of milli-q water, 10 $\mu$ L of 5x Phusion HF Buffer (Thermo Scientific), 5 $\mu$ L of 2.5mM dNTPs, 3 $\mu$ L of 10 $\mu$ M forward primer, 3 $\mu$ L of 10 $\mu$ M reverse primer, 0.5 $\mu$ L of Phusion DNA polymerase (Thermo Scientific) and 0.5 $\mu$ L of the plasmid acting as the genetic material source. 10 $\mu$ L of 6x loading dye (2 $\mu$ L of loading dye for every 10 $\mu$ L of reaction) was added to the reaction after the PCR program was complete and 10 $\mu$ L of the dyed reaction was placed in a 1% Agarose A (Bio Pioneer) gel and run at ~90mV for 10-15 minutes for gel electrophoresis. If the length of the band looked appropriate, the rest of the reaction was purified using a NucleoSpin Gel and PCR Clean-Up Kit (Macherey-Nagel) and DNA concentrations and quality measured with a Nandodrop 1000 Spectrophotometer (Thermo Scientific) before use in USER cloning (Table 4). The USER cloning reactions contained 7.5 $\mu$ L of 200131 35S:USER-

GFP PaCI, 0.5 $\mu$ L of the purified fragment of the GOI, 1 $\mu$ L of 10x CutSmart Buffer (New England BioLabs), and 1 $\mu$ L of USER Enzyme (New England BioLabs). Reactions were incubated at 37 $^{\circ}$ C for 25 minutes then 25 $^{\circ}$ C for 25 minutes then transformed into competent cells from the *E. coli* strain JM109 and plated onto a lysogeny broth (LB) plate with 100 $\mu$ g/mL of Carbenicillin. After being left in 37 $^{\circ}$ C overnight, colonies were purified using the GeneJET Plasmid Miniprep Kit (Thermo Scientific) and submitted to Retrogen for sequencing to ensure the GOIs had the correct sequences before being amplified (Table 3). The same 50 $\mu$ L amplification reaction mixture was used but with a forward primer specific to the GOI and pGC1, a reverse primer specific to Nos, and newly purified plasmids as the source of genetic material. Gel electrophoresis, DNA purification, and nanodrop analysis were all performed using the same steps previously mentioned for amplification before the purified GOIs were used in SLiCE cloning. For SLiCE cloning, the reactions contained 4 $\mu$ L of 170523 pGC1:Nos PC1300 Bam, 4 $\mu$ L of the purified GOI-GFP fragment, 1 $\mu$ L of 10x SLiCE buffer prepared as previously described (Motohashi, 2015), and 1 $\mu$ L of SLiCE enzyme prepared as described previously (Motohashi, 2015). These reactions were incubated for 30 minutes at 37 $^{\circ}$ C before being transformed into the competent *E. coli* cell strain JM109 and plated onto an LB plate with 100 $\mu$ g/mL of Kanamycin. Colonies that formed after the plate was incubated at 37 $^{\circ}$ C overnight were purified using the GeneJET Plasmid Miniprep Kit (Thermo Scientific) and sequenced by Retrogen. Once the genetic sequencing was confirmed to be correct these plasmids were used for the transformation of *Agrobacterium tumefaciens* competent cells.



### 1.7 *Agrobacterium tumefaciens* transformation.

The vectors transformed into *A. tumefaciens* cells contained a guard cell specific promoter (*pGCI*) on the 5' end with a GFP tag placed at the 3' end. To start, competent cells were removed from a -80°C freezer and left in room temperature for 3 minutes to thaw. 5µl of the *E. coli* plasmid with the GOI was added to the competent cells before the microfuge tube containing the sample was thrown into liquid nitrogen to flash freeze it. The sample was removed and incubated at 37°C for ten minutes then 400µl of lysogeny broth (LB) medium was added before placing the tube on a shaker inside a 28°C room for two hours. After two hours the sample was plated onto an LB plate with 50µg/mL Gentamicin and 100µg/mL of Kanamycin and placed back into the 28°C room for two days before being checked for any colony growth. Colonies were selected for use in transforming *A. thaliana* background plants via floral dipping.

### *1.8 Arabidopsis thaliana transformation with Agrobacterium vectors via floral dipping.*

The first step to this three-day process was to make a starting culture made of 3mL of autoclaved lysogeny broth (LB) medium with 3 $\mu$ l of 50 $\mu$ g/mL Gentamicin and 3 $\mu$ l of 100 $\mu$ g/mL Kanamycin within a 10 mL glass test tube in a sterile environment. A colony was taken from a plate and placed inside the test tube, a cap was added, and the test tube was placed on a shaker within a room heated to 28°C overnight. The next day, this culture was upscaled. A 500mL glass container is filled with 200mL of LB medium was autoclaved and once it cooled, 200 $\mu$ l of 50 $\mu$ g/mL Gentamicin and 200 $\mu$ l of 100 $\mu$ g/mL Kanamycin was added so anything that was not the bacteria with the resistance genes could not grow. From the previous day's culture, 1mL was added into the 200mL of LB medium and the container was placed back on the shaker within the 28°C room overnight. On the third day, the 200mL solution was centrifuged at 4000 rotations per minute (RPM) for 10 minutes at room temperature. The supernatant was discarded and 200 mL of an autoclaved solution of ½ Murashige and Skooge (Sigma) with 5% sucrose was combined with the centrifuged cells and mixed until the mixture was homogenized. 40 $\mu$ l of Bioworld SILWET L-77 (Fisher Scientific) was added to the solution then poured into a container. Before the dipping began, all plants (~4 weeks old) had all fertilized flowers/seed containers removed with scissors so only unopened buds and unpollinated flowers remained. These samples were then dipped into the solution for 50 seconds, removed for 30 seconds, and dipped again for 50 seconds before being placed on their sides inside a tray. Once all the samples had been dipped and placed in the tray, the tray is wrapped in aluminum foil and placed in the growth room to incubate for two days. Once the incubation period was over, the foil was removed, samples placed right side up, and water was added to the tray so regular growth conditions were continued until the plants were old enough to have their seeds harvested for selection assays.

### *1.9 Confocal microscopy imaging.*

When GFP vector-expressing candidate plant samples were 2-3 weeks old, a small flat piece of a leaf was removed with scissors. This slice was then placed upside down onto a droplet of 30% glycerol on 25 x 75 x 1mm Premium Clipped Corner Frosted Microscope Slides (Fisher Scientific) and covered with a 12-545-102 Microscope Cover Glass (Fisherbrand). This sample was examined at x100 using a spinning-disk confocal-microscope that was set up as previously described (Paredes et al., 2006) using both brightfield and a GFP filter in conjunction with a Model HB-10103AF mercury lamp (Nikon) to see if there was any strong fluorescence within the guard cells independent from general autofluorescence levels observed in stomata. Images were taken with the Version 7.7.7.0 MetaMorph program with exposure set on 4 second intervals and image processing to isolate the green color was done with ImageJ version 1.53f51.

### *1.10 Li-COR gas exchange experiments.*

Plants grown specifically for use in stomatal conductance experiments were grown in individual pots with sterilized potting soil and grown in a plant growth chamber (AR-41L2; Percival Scientific, Perry, Iowa, USA). The growth chamber settings were set to 12 hours of light and 12 hours of dark with  $\sim 111 \mu\text{mol m}^{-2} \text{s}^{-1}$  light,  $\text{CO}_2$  levels  $\sim 600$  p.p.m., 55-65% relative humidity, and a temperature of  $21^\circ\text{C}$ . Analyses were done using a portable gas-exchange system (LI-6400 or LI-6400XT; LI-COR, Lincoln, Nebraska, USA) each with their own LED light source that was set to  $150 \mu\text{mol m}^{-2} \text{sec}^{-1}$ . The relative humidity for all experiments was monitored so that the value remained between 60-70%, the air flow was set to  $400 \mu\text{mol sec}^{-1}$ , and the leaf temperature within the chamber was set to  $21^\circ\text{C}$ . Before each stomatal response experiment began, each leaf sample was given time to acclimate to the environment within the chamber where  $\text{CO}_2$  levels were set to  $\sim 400$  p.p.m. until the stomatal conductance was stable, this usually took about one hour. Then, after the program began, the sample's stomatal conductance was recorded every 30 seconds until the program was complete. Both programs used began with carbon dioxide levels of 400 p.p.m. to simulate the approximate current ambient levels of the atmosphere, followed by 800 p.p.m. for high carbon dioxide levels, and concluded with 150 p.p.m. for low carbon dioxide levels.

## WORKS CITED

- Ainsworth, Elizabeth A., and Alistair Rogers. "The Response of Photosynthesis and Stomatal Conductance to Rising [CO<sub>2</sub>]: Mechanisms and Environmental Interactions." *Plant, Cell & Environment* 30, no. 3 (2007): 258–70. <https://doi.org/10.1111/j.1365-3040.2007.01641.x>.
- Assmann, S. M., L. Simoncini, and J. I. Schroeder. "Blue light activates electrogenic ion pumping in guard cell protoplasts of *Vicia faba*." *Nature* 318.6043 (1985): 285-287. <https://doi.org/10.1038/318285a0>
- Bongaarts, John. "Human population growth and the demographic transition." *Philosophical Transactions of the Royal Society B: Biological Sciences* 364.1532 (2009): 2985-2990. <https://doi.org/10.1098/rstb.2009.0137>
- Callendar, Guy Stewart. "The artificial production of carbon dioxide and its influence on temperature." *Quarterly Journal of the Royal Meteorological Society* 64.275 (1938): 223-240. <https://doi.org/10.1002/qj.49706427503>
- Darwin, Francis. "IX. Observations on stomata." *Philosophical Transactions of the Royal Society of London. Series B, Containing Papers of a Biological Character* 190 (1898): 531-621. <https://doi.org/10.1098/rstb.1898.0009>
- Gray, Sharon B., Orla Dermody, Stephanie P. Klein, Anna M. Locke, Justin M. McGrath, Rachel E. Paul, David M. Rosenthal, Ursula M. Ruiz-Vera, Matthew H. Siebers, Reid Strellner, Elizabeth A. Ainsworth, Carl J. Bernacchi, Stephen P. Long, Donald R. Ort, and Andrew D. B. Leaky. "Intensifying drought eliminates the expected benefits of elevated carbon dioxide for soybean." *Nature Plants* 2.9 (2016): 1-8. <https://doi.org/10.1038/nplants.2016.132>
- Gomi, Kenji, Daisuke Ogawa, Shinpei Katou, Hiroshi Kamada, Nobuyoshi Nakajima, Hikaru Saji, Takashi Soyano, Michiko Sasabe, Yasunori Machida, Ichiro Mitsuhashi, Yuko Ohashi, and Shigemi Seo. "A mitogen-activated protein kinase NtMPK4 activated by SIPKK is required for jasmonic acid signaling and involved in ozone tolerance via stomatal movement in tobacco." *Plant and Cell Physiology* 46.12 (2005): 1902-1914. <https://doi.org/10.1093/pcp/pci211>
- Gull, Audil, Ajaz Ahmad Lone, and Noor Ul Islam Wani. "Biotic and abiotic stresses in plants." *Abiotic and biotic stress in plants* (2019): 1-19.

- Hashimoto-Sugimoto, Mimi, Juntaro Negi, Keina Monda, Takumi Higaki, Yasuhiro Isogai, Toshiaki Nakano, Seiichiro Hasezawa, and Koh Iba. "Dominant and Recessive Mutations in the Raf-like Kinase HT1 Gene Completely Disrupt Stomatal Responses to CO<sub>2</sub> in Arabidopsis." *Journal of Experimental Botany* 67, no. 11 (May 2016): 3251–61. <https://doi.org/10.1093/jxb/erw134>.
- Hatfield, Jerry L. "Increased temperatures have dramatic effects on growth and grain yield of three maize hybrids." *Agricultural & Environmental Letters* 1.1 (2016): 150006. <https://doi.org/10.2134/ael2015.10.0006>
- Hettenhausen, Christian, Ian T. Baldwin, and Jianqiang Wu. "Silencing MPK4 in *Nicotiana attenuata* enhances photosynthesis and seed production but compromises abscisic acid-induced stomatal closure and guard cell-mediated resistance to *Pseudomonas syringae* pv tomato DC3000." *Plant Physiology* 158.2 (2012): 759-776. <https://doi.org/10.1104/pp.111.190074>
- Hetherington, Alistair M., and F. Ian Woodward. "The Role of Stomata in Sensing and Driving Environmental Change." *Nature* 424, no. 6951 (August 2003): 901–8. <https://doi.org/10.1038/nature01843>.
- Hewett-Emmett, David, and Richard E. Tashian. "Functional diversity, conservation, and convergence in the evolution of the  $\alpha$ -,  $\beta$ -, and  $\gamma$ -carbonic anhydrase gene families." *Molecular phylogenetics and evolution* 5.1 (1996): 50-77. <https://doi.org/10.1006/mpev.1996.0006>
- Hiyama, Asami, Atsushi Takemiya, Shintaro Munemasa, Eiji Okuma, Naoyuki Sugiyama, Yasuomi Tada, Yoshiyuki Murata, and Ken-ichiro Shimazaki. "Blue Light and CO<sub>2</sub> Signals Converge to Regulate Light-Induced Stomatal Opening." *Nature Communications* 8, no. 1 (November 3, 2017): 1284. <https://doi.org/10.1038/s41467-017-01237-5>.
- Hörak, Hanna, Maija Sierla, Kadri Töldsepp, Cun Wang, Yuh-Shuh Wang, Maris Nuhkat, Ervin Valk, Priit Pechter, Ebe Merilo, Jarkko Salojärvi, Kirk Overmyer, Mart Loog, Mikael Brosche, Julian I. Schroeder, Jaakko Kangasjarvi, Hannes Kollist. "A Dominant Mutation in the HT1 Kinase Uncovers Roles of MAP Kinases and GHR1 in CO<sub>2</sub>-Induced Stomatal Closure." *The Plant Cell* 28, no. 10 (October 1, 2016): 2493–2509. <https://doi.org/10.1105/tpc.16.00131>.
- Hsu, Po-Kai, Yohei Takahashi, Shintaro Munemasa, Ebe Merilo, Kristiina Laanemets, Rainer Waadt, Dianne Pater, Hannes Kollist, and Julian I. Schroeder. "Abscisic acid-independent stomatal CO<sub>2</sub> signal transduction pathway and convergence of CO<sub>2</sub> and ABA signaling downstream of OST1 kinase." *Proceedings of the National Academy of Sciences* 115.42 (2018): E9971-E9980. <https://doi.org/10.1073/pnas.1809204115>

- Hu, Honghong, Aurélien Boisson-Dernier, Maria Israelsson-Nordström, Maik Böhmer, Shaowu Xue, Amber Ries, Jan Godoski, Josef M. Kuhn, and Julian I. Schroeder. "Carbonic anhydrases are upstream regulators of CO<sub>2</sub>-controlled stomatal movements in guard cells." *Nature cell biology* 12.1 (2010): 87-93 87–93 (2010).  
<https://doi.org/10.1038/ncb2009>
- IPCC, 2014: Summary for Policymakers. In: *Climate Change 2014: Mitigation of Climate Change. Contribution of Working Group III to the Fifth Assessment Report of the Intergovernmental Panel on Climate Change* [Edenhofer, O., R. Pichs-Madruga, Y. Sokona, E. Farahani, S. Kadner, K. Seyboth, A. Adler, I. Baum, S. Brunner, P. Eickemeier, B. Kriemann, J. Savolainen, S. Schlömer, C. von Stechow, T. Zwickel and J.C. Minx (eds.)]. Cambridge University Press, Cambridge, United Kingdom and New York, NY, USA.
- Jakobson, Liina, Lauri Vaahtera, Kadri Töldsepp, Maris Nuhkat, Cun Wang, Yuh-Shuh Wang, Hanna Hõrak, Ervin Valk, Priit Pechter, Yana Sindarovska, Jing Tang, Chuanlei Xiao, Yang Xu, Ulvi Gerst Talas, Alfonso T. Garcí ´a-Sosa, Saijaliisa Kangasja ´rvi, Uko Maran, Mairo Remm, M. Rob G. Roelfsema, Honghong Hu, Jaakko Kangasja ´rvi, Mart Loog, Julian I. Schroeder, Hannes Kollist, Mikael Brosche. "Natural Variation in Arabidopsis Cvi-0 Accession Reveals an Important Role of MPK12 in Guard Cell CO<sub>2</sub> Signaling." *PLOS Biology* 14, no. 12 (December 6, 2016): e2000322.  
<https://doi.org/10.1371/journal.pbio.2000322>.
- Jones, Hamlyn G. "Application of thermal imaging and infrared sensing in plant physiology and ecophysiology." *Advances in botanical research* 41 (2004): 107-163.  
[https://doi.org/10.1016/S0065-2296\(04\)41003-9](https://doi.org/10.1016/S0065-2296(04)41003-9)
- Laanemets, Kristiina, Yong-Fei Wang, Ove Lindgren, Juyou Wu, Noriyuki Nishimura, Stephen Lee, Daniel Caddell, Ebe Merilo, Mikael Brosche, Kale Kilk, Ursel Soomets, Jaakko Kangasjrvi, Julian I. Schroeder, and Hannes Kollist. "Mutations in the SLAC 1 anion channel slow stomatal opening and severely reduce K<sup>+</sup> uptake channel activity via enhanced cytosolic [Ca<sup>2+</sup>] and increased Ca<sup>2+</sup> sensitivity of K<sup>+</sup> uptake channels." *New Phytologist* 197.1 (2013): 88-98. <https://doi.org/10.1111/nph.12008>
- Marten, Holger, Taekyung Hyun, Kenji Gomi, Shigemi Seo, Rainer Hedrich, and M. Rob G. Roelfsema. "Silencing of NtMPK4 Impairs CO<sub>2</sub>-Induced Stomatal Closure, Activation of Anion Channels and Cytosolic Casignals in Nicotiana Tabacum Guard Cells." *The Plant Journal: For Cell and Molecular Biology* 55, no. 4 (August 2008): 698–708.  
<https://doi.org/10.1111/j.1365-313X.2008.03542.x>.
- Movahedi, Mahsa, Nicholas Zoulias, Stuart A. Casson, Peng Sun, Yun-Kuan Liang, Alistair M. Hetherington, Julie E. Gray, and Caspar C. C. Chater. "Stomatal responses to carbon dioxide and light require abscisic acid catabolism in Arabidopsis." *Interface Focus* 11.2 (2021): 20200036. <https://doi.org/10.1098/rsfs.2020.0036>

- Mustilli, Anna-Chiara, Sylvain Merlot, Alain Vavasseur, Francesca Fenzi, and Jérôme Giraudat. "Arabidopsis OST1 protein kinase mediates the regulation of stomatal aperture by abscisic acid and acts upstream of reactive oxygen species production." *The Plant Cell* 14.12 (2002): 3089-3099. <https://doi.org/10.1105/tpc.007906>
- Parry, Martin. "The implications of climate change for crop yields, global food supply and risk of hunger." (2007).
- Santer, Benjamin D., K.E. Taylor, T. M. L. Wigley, T. C. Johns, P. D. Jones, D. J. Karoly, J. F. B. Mitchell, A. H. Oort, J. E. Penner, V. Ramaswamy, M. D. Schwarzkopf, and S. Tett. "A search for human influences on the thermal structure of the atmosphere." *Nature* 382.6586 (1996): 39-46. <https://doi.org/10.1038/382039a0>
- Schroeder, J. I., R. Hedrich, and J. M. Fernandez. "Potassium-selective single channels in guard cell protoplasts of *Vicia faba*." *Nature* 312.5992 (1984): 361-362. <https://doi.org/10.1038/312361a0>
- Schroeder, Julian I., Klaus Raschke, and Erwin Neher. "Voltage dependence of K<sup>+</sup> channels in guard-cell protoplasts." *Proceedings of the National Academy of Sciences* 84.12 (1987): 4108-4112. <https://doi.org/10.1073/pnas.84.12.4108>
- Shim, Dana, Kyu-Jong Lee, and Byun-Woo Lee. "Response of phenology-and yield-related traits of maize to elevated temperature in a temperate region." *The Crop Journal* 5.4 (2017): 305-316. <https://doi.org/10.1016/j.cj.2017.01.004>
- Takahashi, Yohei, Krystal Bosmans, Po-Kai Hsu, Karnelia Paul, Chung-Yueh Yeh, Yuh-Shuh Wang, Dimitry Yarmolinsky, Maija Sierla, Triin Vahisalu, Jaakko Kangasjarvi, Hannes Kollist, Li Zhang, Thien Trac, and Julian I. Schroeder. "Stomatal CO<sub>2</sub>/bicarbonate Sensor Consists of Two Interacting Protein Kinases, Raf-like HT1 and non-kinase-activity requiring MPK12/MPK4" **[Unpublished]**
- Töldsepp, Kadri, Jingbo Zhang, Yohei Takahashi, Yana Sindarovska, Hanna Hörak, Paulo H. O. Cecilato, Kaspar Koolmeister, Yuh-Shuh Wang, Lauri Vaahtera, Liina Jakobson, Chung-Yueh Yeh, Jiyoun Park, Mikael Brosche, Hannes Kollist, and Julian I. Schroeder. "Mitogen- Activated Protein Kinases MPK4 and MPK12 Are Key Components Mediating CO<sub>2</sub> -Induced Stomatal Movements." *The Plant Journal: For Cell and Molecular Biology* 96, no. 5 (December 2018): 1018–35. <https://doi.org/10.1111/tpj.14087>.
- USGCRP, 2017: *Climate Science Special Report: Fourth National Climate Assessment, Volume I* [Wuebbles, D.J., D.W. Fahey, K.A. Hibbard, D.J. Dokken, B.C. Stewart, and T.K. Mayock (eds.)]. U.S. Global Change Research Program, Washington, DC, USA, 470 pp, doi: 10.7930/J0J964J6



- Webb, Alex AR, Martin R. McAinsh, Terry A. Mansfield, Alistair M. Hetherington. "Carbon dioxide induces increases in guard cell cytosolic free calcium." *The Plant Journal* 9.3 (1996): 297-304. <https://doi.org/10.1046/j.1365-313X.1996.09030297.x>
- Xue, Shaowu, Honghong Hu, Amber Ries, Ebe Merilo, Hannes Kollist, and Julian I Schroeder. "Central Functions of Bicarbonate in S-Type Anion Channel Activation and OST1 Protein Kinase in CO<sub>2</sub> Signal Transduction in Guard Cell." *The EMBO Journal* 30, no. 8 (April 20, 2011): 1645–58. <https://doi.org/10.1038/emboj.2011.68>.
- Yang, Yingzhen, Alex Costa, Nathalie Leonhardt, Robert S Siegel, and Julian I. Schroeder. "Isolation of a strong Arabidopsis guard cell promoter and its potential as a research tool." *Plant Methods* 4.1 (2008): 1-15. <https://doi.org/10.1186/1746-4811-4-6>
- Zhang, Jingbo, Paulo De-oliveira-Ceciliato, Yohei Takahashi, Sebastian Schulze, Guillaume Dubeaux, Felix Hauser, Tamar Azoulay-Shemer, Kadri Tõldsepp, Hannes Kollist, Wouter-Jan Rappel, and Julian I. Schroeder. "Insights into the molecular mechanisms of CO<sub>2</sub>-mediated regulation of stomatal movements." *Current Biology* 28.23 (2018): R1356-R1363. <https://doi.org/10.1016/j.cub.2018.10.015>